

Spin coherence of holes and electrons in undoped CdTe/(Cd,Mg)Te quantum wells

E. A. Zhukov,^{1,2} D. R. Yakovlev,^{1,3} M. Gerbrach,¹ G. V. Mikhailov,³ G. Karczewski,⁴ T. Wojtowicz,⁴ J. Kossut,⁴ and M. Bayer¹

¹*Experimentelle Physik II, Technische Universität Dortmund, 44221 Dortmund, Germany*

²*Faculty of Physics, M. V. Lomonosov Moscow State University, 119992 Moscow, Russia*

³*A. F. Ioffe Physico-Technical Institute, Russian Academy of Sciences, 194021 St. Petersburg, Russia*

⁴*Institute of Physics, Polish Academy of Sciences, PL-02668 Warsaw, Poland*

(Received 29 January 2009; revised manuscript received 30 March 2009; published 24 April 2009)

The coherent spin dynamics of electrons and holes in an undoped CdTe/(Cd,Mg)Te quantum well structure was studied by time-resolved pump-probe Kerr rotation technique using resonant excitation of the charged exciton (trion) state. Long-living spin coherence of electrons (up to 10 ns) and holes (up to 500 ps) was measured. The unusual observation of long-living spin beats from both types of carriers in parallel is explained by coexistence of resident electrons and holes which are separated spatially in the quantum well plane. This conclusion is confirmed by experiments where type and concentration of resident carriers are tuned by above-barrier illumination.

DOI: [10.1103/PhysRevB.79.155318](https://doi.org/10.1103/PhysRevB.79.155318)

PACS number(s): 78.55.Cr

I. INTRODUCTION

The spin dynamics of carriers in semiconductor quantum wells (QWs) and quantum dots has attracted recently considerable attention due to demonstration of a wealth of unexpected physics and also potential application in spintronics and quantum information.¹⁻³ Coherent spin dynamics is a very active field of ongoing research, in particular with respect to not only generating and measuring spin coherence but also manipulating it optically while coherence is retained. These studies have mostly focused on the electron spin while information about hole spin properties is very limited. However the hole plays an important role in optical generation and coherent control protocols of electron spin coherence via resonant pumping of the charged electron-hole complex (trion).^{4,5}

The hole spin relaxation differs drastically from that of the electron: on one hand the spin-orbit interaction is much stronger and provides spin relaxation much more sufficient for free holes than for free electrons. On the other hand the hyperfine interaction with the nuclear spins, which is inherent for localized electrons,^{6,7} is not significant for holes.⁸ Therefore long spin relaxation and spin coherence times are expected for localized holes, which have been confirmed by recent reports for the longitudinal spin relaxation time in quantum dots.⁹⁻¹² A very recent theoretical report suggests, however, that the hyperfine interaction for holes can be sufficiently strong in quantum dots to provide the hole spin decoherence.¹³ These few examples show that we are still at the beginning of the road toward a comprehensive understanding of hole spin dynamics in nanostructures.

For quantum well structures, the hole spin dynamics has been mainly studied for GaAs-based samples. Earlier reports exploited the optical orientation technique, where the polarized photoluminescence (PL) is measured either time integrated or time resolved.¹⁴⁻¹⁸ Experimental studies addressed the longitudinal spin relaxation time T_1 (Refs. 14-16) and the spin dephasing time T_2^* via hole spin quantum beats.¹⁸ The reported relaxation times vary from 4 ps (Ref. 14) up to

1 ns (Refs. 16 and 18) demonstrating strong dependencies on doping density and excitation energy. Recently the dephasing time of the hole spin coherence was examined by the pump-probe Kerr rotation technique.¹⁹ Long times up to 650 ps were obtained for localized holes, which however shorten drastically with increasing temperature, most likely due to hole delocalization. A new technique based on the resonant spin amplification method was suggested recently for studying the hole spin dynamics.²⁰ It allowed to measure hole spin relaxation times T_1 up to 2 ns in *n*-type (In,Ga)As/GaAs QWs, while the hole lifetimes were limited to 120 ps by trion recombination. It would be important to extend these studies to other material systems, e.g., QWs based on II-VI semiconductors, in order to highlight the generality of spin relaxation origins or to reveal deviations from already reported observations.

In this paper we present time-resolved pump-probe Kerr rotation studies of the spin coherence of holes and electrons in a nominally undoped CdTe/(Cd,Mg)Te quantum well structure, for which type and concentration of resident carriers can be tuned by above-barrier illumination. We observed long-living spin coherence both of holes and electrons at low temperatures when the resident carriers are localized by potential fluctuations induced by QW width variations. We found also a regime where resident electrons and holes coexist spatially separated in the QW. In this case Kerr rotation signals from both types of carriers can be detected at time delays considerably exceeding the times of exciton and trion recombination.

II. EXPERIMENTAL

The studied CdTe/Cd_{0.63}Mg_{0.37}Te quantum well structure (090505AC) was grown by molecular-beam epitaxy on a (100)-oriented GaAs substrate followed by a 4 μm Cd_{0.75}Mg_{0.25}Te buffer layer. The structure contains a 20-nm-thick single CdTe QW separated from the buffer layer by a 150-nm-thick Cd_{0.63}Mg_{0.37}Te barrier and from the surface by a 120-nm-thick Cd_{0.63}Mg_{0.37}Te barrier. The sample is nomi-

nally undoped but due to residual impurities and charge redistribution to surface states the QW at low temperature contains resident holes. The concentration of this two-dimensional hole gas (2DHG) does not exceed 10^{10} cm $^{-2}$.²¹ Illumination with photon energies exceeding the band gap of Cd $_{0.63}$ Mg $_{0.37}$ Te barriers of 2.26 eV provides additional electrons in the QW, which allows us to tune the hole density and even invert the type of resident carriers from holes to electrons.^{19,22} The achievable density of the two-dimensional electron gas (2DEG) was a few 10^9 cm $^{-2}$.

Several experimental techniques were used in our spin dynamics studies. Continuous-wave (cw) PL and reflectivity measurements were performed at temperatures of 0.35 and 4.2 K and in magnetic fields B up to 15 T applied parallel to the structure growth axis, which is chosen as z axis, $\mathbf{B} \parallel \mathbf{z}$ (Faraday geometry). The circular polarization degree of PL was detected, which allows us to identify negatively (T^-) and positively (T^+) charged trions and thereby identify the dominant type of resident carriers. Below-barrier photoexcitation at an energy of 1.664 eV (wavelength of 745 nm) was performed by a Ti:sapphire laser. For above-barrier illumination we used a cw yttrium aluminum garnet (YAG) laser emitting photons at 2.33 eV (532 nm). Reflectivity spectra were measured using a halogen lamp, the spectrum of which was shaped by a RG780 long-pass optical filter in order to exclude above-barrier illumination and related effects on the resident carriers.

The recombination dynamics of excitons and trions was investigated by time-resolved PL. A Ti:sapphire laser generating spectrally narrow pulses with a duration of 1.5 ps at a repetition frequency of 75.6 MHz was used for excitation. The signal was detected with a synchroscan streak camera connected to a 0.5 m spectrometer. The time resolution was about 12 ps. The experiments were performed at zero magnetic field and at a temperature $T=1.9$ K with the sample immersed in pumped liquid helium.

A time-resolved pump-probe Kerr rotation technique was used to study the coherent spin dynamics of resident holes and electrons.^{19,23} As excitation source again a pulsed Ti:sapphire laser, whose beam was split in pump and probe beams, was used. The pump beam was circularly polarized by a photoelastic modulator operated at 50 kHz frequency. The probe beam was linearly polarized. The angle of the polarization plane rotation for the reflected probe beam, which was sent through a Glan-Thompson polarization sensitive beam splitter, was measured by a balanced photodetector interfaced by a lock-in amplifier. The time delay between pump and probe pulses was varied up to 7 ns by a mechanical delay line. The spectral width of the 1.5 ps laser pulses does not exceed 1 meV, which is smaller than the trion binding energy of 2.2 meV, and therefore allows selective excitation of the trion or exciton states. The measurements were performed in magnetic fields up to 6 T applied perpendicular to the structure growth axis, $\mathbf{B} \perp \mathbf{z}$ (Voigt geometry), and for sample temperatures varied from 1.9 to 25 K.

The Kerr rotation technique was used in two regimes. For degenerate Kerr rotation, denoted as one-color experiment in the following, the pump and probe beams had the same photon energy as they originated from a single laser. For nondegenerate Kerr rotation, a two-color experiment, the setup was

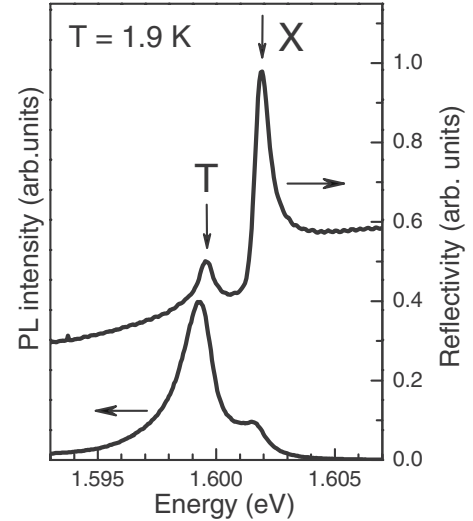


FIG. 1. Photoluminescence and reflectivity spectra of a 20-nm-thick CdTe/Cd $_{0.63}$ Mg $_{0.37}$ Te QW structure. Below-barrier excitation with a photon energy of 1.664 eV is used for PL. The exciton (X) and trion (T) resonances are marked by arrows.

extended by a second Ti:sapphire laser synchronized with the first one. This allowed us to tune the energies of the pump and probe beams independently.

Due to splitting of the heavy-hole and light-hole states in QWs the heavy-hole g factor is strongly anisotropic. Its in-plane component is close to zero, $g_{h,xy} \sim 0$, and therefore it is difficult to determine it by hole spin beats. Deviation of $g_{h,xy}$ from zero value is due to mixing of the heavy-hole and light-hole states and is controlled by structural parameters, such as well width, barrier height, and strain in the QW layer. To enhance visibility of the hole spin beats in the Kerr rotation experiment we tilted the magnetic field slightly out of the plane by an angle $\vartheta \approx 3.5^\circ$. This increases the hole g factor by mixing the in-plane component ($g_{h,xy}$) with the one parallel to the QW growth axis ($g_{h,z}$),

$$g_h(\vartheta) = \sqrt{g_{h,z}^2 \sin^2 \vartheta + g_{h,xy}^2 \cos^2 \vartheta}. \quad (1)$$

For the studied QW $g_{h,z} = -1.70$ (Ref. 24) in weak magnetic fields so that $g_h(\vartheta \approx 3.5^\circ)$ is considerably increased compared to the in-plane component. For conduction band electrons the g -factor anisotropy does not exceed 6% (Ref. 25) so that $g_e(\vartheta \approx 3.5^\circ) = g_{e,xy}$ with high accuracy.

III. EXPERIMENTAL RESULTS AND DISCUSSION

Photoluminescence and reflectivity spectra of the studied QW structure are shown in Fig. 1. Two spectral lines corresponding to the heavy-hole exciton (X) and trion (T) emission are clearly seen in the PL spectrum. They are separated by 2.2 meV, the trion binding energy.²⁶ The broadening of the lines is mainly due to exciton and trion localization in QW width fluctuations. The low energy tail of the trion line is contributed by shake-up processes accompanying the trion recombination.²⁷

The exciton and trion resonances are also clearly seen in the reflectivity spectrum. The oscillator strength of the trion

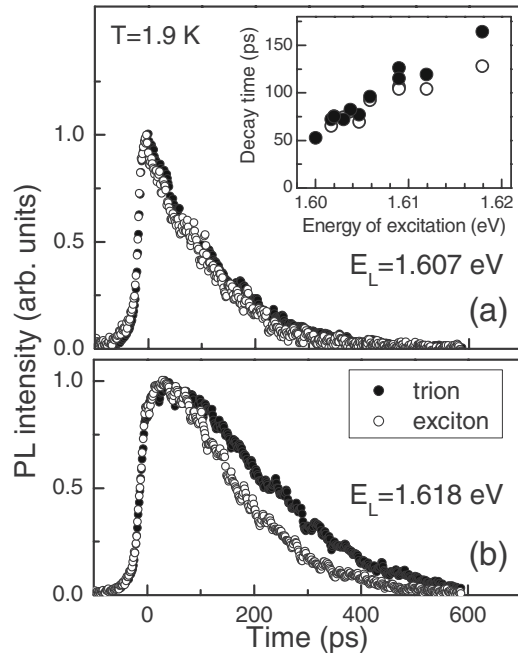


FIG. 2. Kinetics of photoluminescence decay of trions (closed circles) and excitons (open circles) for different photon energies of excitation E_L . Intensities are normalized by the maximum for the corresponding line. Decay time dependence on excitation energy is given in the inset.

resonance, which is proportional to the concentration of resident carriers,²⁸ is about 1 order of magnitude smaller than the exciton oscillator strength. This allows us to evaluate the resident carrier concentration and estimate that it does not exceed 10^{10} cm⁻². However, the spectra measured at zero magnetic field do not contain information about the type of resident carriers, as the binding energies of positively and negatively charged trions are rather close to each other,²² and they also vary with QW width and barrier height.²⁹ Magneto-optical experiments are required to identify the resident carrier type. We will show in Sec. III B that in the studied sample the trion PL line is dominated by positively charged trions for below-barrier excitation, and therefore holes are the resident carriers.

A. Recombination kinetics of excitons and trions

Results on the recombination dynamics of excitons and trions measured with the streak camera are given in Fig. 2. The excitation energies were varied from 1.600 eV, nearly resonant with the trion, up to 1.618 eV. Trions and excitons demonstrate very similar behaviors. The decay time under resonant excitation of 50 ps can be attributed to the radiative recombination time of trions and excitons generated within the radiative cone, where their wave vectors are transferred to the photons during recombination. The decay time increases steadily with detuning the excitation energy from the resonance condition and approaches value around 150 ps at 1.618 eV excitation energy. This increased time is required because of exciton and trion thermalization (for more details see Ref. 23).

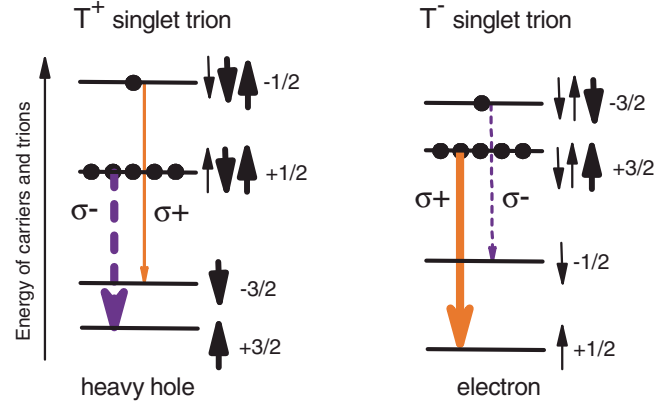


FIG. 3. (Color online) Scheme of optical transitions in a 20-nm-thick CdTe/Cd_{0.63}Mg_{0.37}Te QW for recombination of positively and negatively charged trions in an external magnetic field (Faraday geometry). Optically active transitions with positive and negative circular polarizations are shown by solid and dashed arrows, respectively. The thick arrows represent the strongest transitions in PL. Initial states for the optical transitions are the trion singlet states and the final states are the resident carriers left after trion recombination. The scheme is shown for the following conditions of electron and hole g factors: $g_{e,z} < 0$, $g_{h,z} < 0$, and $|g_{e,z}| > |g_{h,z}|$. Thin short arrows indicate the electron spins with orientation $\pm 1/2$, while thick short arrows give the spins of heavy holes $\pm 3/2$.

B. Optical tuning of type and density of resident carriers

Magneto-optics and in particular polarized PL in magnetic fields applied in Faraday geometry are powerful tools to identify the origin of the trion transition (see e.g., Refs. 22 and 26). In the case when the electron and hole g factors have the same sign, the emission from the singlet state of the negatively (T^-) and positively (T^+) charged trions has opposite polarizations. Thereby they can be unambiguously identified, and this gives us information on the type of the resident carriers. This is also the case for the studied 20-nm-thick CdTe/Cd_{0.63}Mg_{0.37}Te QW, where the electron g factor $g_{e,z} = -1.70$ and the hole g factor $g_{h,z}$ varies from -1.70 to -1.00 in the magnetic field range of 0–15 T. The B dependence of $g_{h,z}$ is due to a change in mixing of heavy-hole and light-hole states by the field. Details of the comprehensive magneto-optical study of this sample will be published elsewhere.²⁴

In Fig. 3 we show the scheme of optical transitions for recombination of positively and negatively charged trions. Number of circles illustrates the dominant population of the trion singlet states for quasiequilibrium conditions after carrier relaxation, and thickness of arrows indicates the intensity of the recombination transitions. One can see that photoluminescence has negative circular polarization for T^+ and is positively polarized for T^- .

The polarization degrees of the trion emission excited below and above the barrier gap are shown in Fig. 4. Experiments were performed in Faraday geometry for two lattice temperatures of 0.35 and 4.2 K. For both temperatures the trion emission under below-barrier excitation is negatively polarized, meaning that it can be attributed to T^+ and holes are the resident carriers in the QW. Under above-barrier ex-

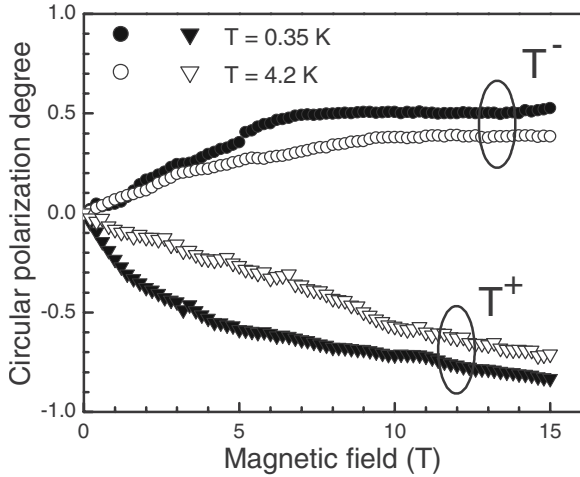


FIG. 4. Magnetic field dependence of circular polarization degree of trion PL measured at two lattice temperatures. Magnetic fields are applied in Faraday geometry. Two excitation energies were used: below-barrier excitation at 1.664 eV (triangles) and above-barrier excitation at 2.33 eV (circles).

citation the polarization degree is positive, which corresponds to T^- emission and resident electrons. Thus the illumination may be used to vary the type of resident carriers in the QW. The stronger polarization for lower lattice temperatures can be explained by better thermalization of the trions between the spin split singlet states.

The experimental results of this section demonstrate that the type and concentration of the resident carriers in the studied structure can be tuned by above-barrier illumination. We will use this tool for studying the spin coherence of both resident holes and electrons.

C. Spin coherence of resident carriers

We turn now to the main focus of the paper related to the carrier spin coherence. Kerr rotation signals measured by the one-color technique on the studied QW are shown in Fig. 5 for different laser excitation energies. The experiments were performed in a magnetic field $B=0.5$ T applied in Voigt geometry. All Kerr signals show fast beats corresponding to spin precession of the electrons with a g -factor value $|g_{e,xy}| = 1.60 \pm 0.01$.^{23,25} For resonant trion excitation an additional contribution with slow oscillation frequency corresponding to a g -factor value of 0.11 ± 0.01 is seen. Details of the g -factor evaluation will be given below when discussing Fig. 8. At short delays this contribution is seen as a drop of the Kerr signal averaged over the fast oscillations to values well below the zero line. We associate these slow oscillations with hole spin precession, in line with previous observations for GaAs/(Al,Ga)As QWs.¹⁹

The striking difference between the Kerr traces in Fig. 5 and those presented in the previous studies is that two contributions to the Kerr rotation signal from the electrons and the holes are visible for time delays exceeding 1 ns, which exceeds by more than 1 order of magnitude the trion recombination time of 50 ps, as measured by time-resolved PL (see Fig. 2). Such coexistence of long-living beats of electrons

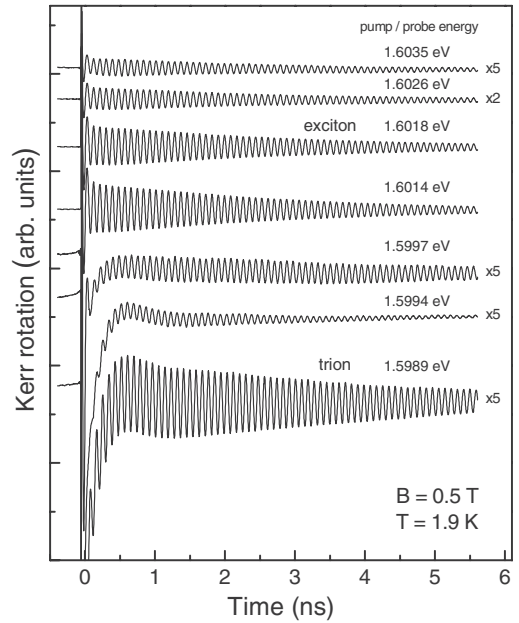


FIG. 5. Kerr rotation signals measured by degenerate pump probe for various excitation energies, $\vartheta \approx 3.5^\circ$.

and holes has not been reported before. In earlier studies only the resident carriers showed long-living spin coherence, while the contribution of the photogenerated carriers decayed within the trion radiative time, as observed in n -type as well as in p -type doped samples.^{19,23} We suggest that in the studied sample we find a coexistence of resident holes and electrons even though the PL data of Fig. 4 show that the concentration of resident holes dominates over the one of the resident electrons. This point will be discussed further in Sec. III D

In Fig. 5 the hole contribution is strong for excitation in the trion resonance and vanishes when the laser is tuned to the exciton resonance or above. As for the degenerate experiments the pump and probe energies coincide, we are not able to conclude from these data whether this behavior is caused by variation in the pump energy or the probe energy. In order to clarify this question we performed two-color pump-probe measurements with the probe energy fixed at the trion resonance and the pump energy scanned across the trion and exciton resonances. The results are given in Fig. 6.

The characteristic feature of the hole contribution, the shift of the center-of-gravity of the Kerr rotation signal at short time delays, is present for all pump energies varied from 1.5994 up to 1.6031 eV. In this experiment the signal is detected on the trion resonance, which is mostly sensitive to the generated hole coherence.^{23,30} We can also conclude from these results that the long-living spin coherence of resident holes can be photogenerated even by pumping at energies of 4 meV above the T^+ resonance. This means that the excitons generated at these energies can capture resident holes and form trions without losing their optical spin orientation. This finding is consistent with previously published results on generation of electron spin coherence in n -type doped QWs.²³

For a quantitative analysis of amplitudes $A_{e(h)}$ and dephasing times $T_{2,e(h)}^*$ of the electron and hole contributions, the Kerr rotation signals were fit by

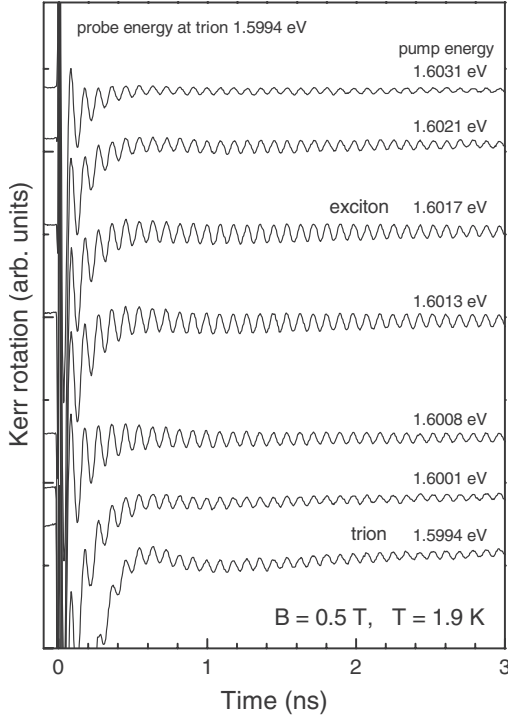


FIG. 6. Kerr rotation signals measured by two-color nondegenerate pump-probe at different pump energies. Probe energy was fixed at the trion resonance, $\vartheta \approx 3.5^\circ$.

$$A(t) = A_e \exp\left(-\frac{t}{T_{2,e}^*}\right) \cos \omega_e t + A_h \exp\left(-\frac{t}{T_{2,h}^*}\right) \cos \omega_h t. \quad (2)$$

This function is a superposition of two exponentially damped oscillatory functions for electrons and holes. $\omega_{e(h)} = \mu_B g_{e(h)} B / \hbar$ are the Larmor frequencies of spin precession about the external magnetic field B and μ_B is the Bohr magneton.

The fit of the experimental data at $B=0.5$ T is given as an example by the bottom trace in Fig. 7. The fit function is shown by the thick gray line together with the experimental signal shown by a thin black line. Hole and electron contributions extracted from the fit are shown separately by the top traces. The hole signal can be followed up to 3 ns, from which a characteristic dephasing time $T_{2,h}^* = 290 \pm 30$ ps can be extracted for the hole spin coherence. Its amplitude A_h is 25 times larger than the one for the electron contribution A_e . The electron dephasing time is $T_{2,e}^* = 4.5 \pm 0.5$ ns, so that the electron beats extend over 6 ns (Fig. 5). The carrier g -factor values obtained from this fit are $|g_{e,xy}| = 1.60 \pm 0.01$ and $|g_h| = 0.11 \pm 0.01$.

Alternatively the characteristic spin precession frequencies in the Kerr rotation signal can be obtained by a Fourier analysis. Fourier transform spectra for $B=0.5$ and 1 T are shown in Fig. 8(a). The narrow peaks at 11.3 and 22.6 GHz correspond to the electron spin beats. Their frequency shifts linearly with magnetic field [see Fig. 8(b)] and can be well described by a Zeeman splitting with $|g_{e,xy}| = 1.60$. The hole contribution is seen as a broad band with maximum at 1.76

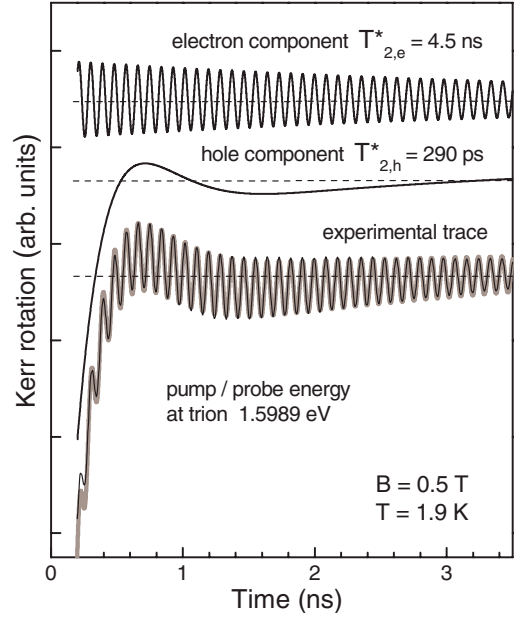


FIG. 7. (Color online) Bottom trace: Kerr rotation signal measured by degenerate pump probe at the trion resonance. Experimental data are given by thin black line and fit by thick gray line. Upper traces were obtained by separating electron and hole contributions from the fit (see text), $\vartheta \approx 3.5^\circ$.

GHz for $B=1$ T. This maximum cannot be well resolved for $B=0.5$ T.

Electron and hole frequencies obtained from Fourier analysis are shown in panel (b) vs magnetic field strength. Linear interpolations of these data give us g -factor values for the carriers, which coincide well with the values obtained by fitting the Kerr rotation signals in Fig. 7 with Eq. (2). Based on the measured hole g factor $|g_h(\vartheta \approx 3.5^\circ)| = 0.11$ and the known value for $g_{h,z} = -1.70$,²⁴ we estimate from Eq. (1) that $|g_{h,xy}| < 0.05$.

In order to obtain the magnetic field dependence of the electron and hole dephasing times Kerr rotation signals under resonant pumping into the trion state were measured for different magnetic fields up to 6 T [Fig. 9(a)]. These times have significantly different values, as the electron dephasing at fixed magnetic field lasts about 20 times longer than the hole one, but show very similar dependence on magnetic field. These dependencies are well described by a $1/B$ law shown in the figure by the solid line. Scales for the electron and hole times are chosen in a way that both dependencies can be compared with the same $1/B$ line. Such a field dependence shows that the spin dephasing is controlled by precession frequency inhomogeneities based on the spread of the carrier g factors,³⁰ which we evaluate as $\Delta g_{e,xy} = 0.008$ and $\Delta g_h(\vartheta \approx 3.5^\circ) = 0.10$, respectively. Note that the variation in the hole g factor is comparable to its magnitude, $\Delta g_h(\vartheta \approx 3.5^\circ) \approx |g_h(\vartheta \approx 3.5^\circ)|$, which is suggested already by the strongly damped single oscillation of the hole beats in Fig. 7.

The longest dephasing times in Fig. 9 measured at $B = 0.25$ T are $T_{2,e}^* = 10.2$ ns and $T_{2,h}^* = 470$ ps, which represent lower limits for the coherence times T_2 of individual carrier spins. The temperature dependence of the hole spin dephasing time is shown in Fig. 9(b). It decreases about three

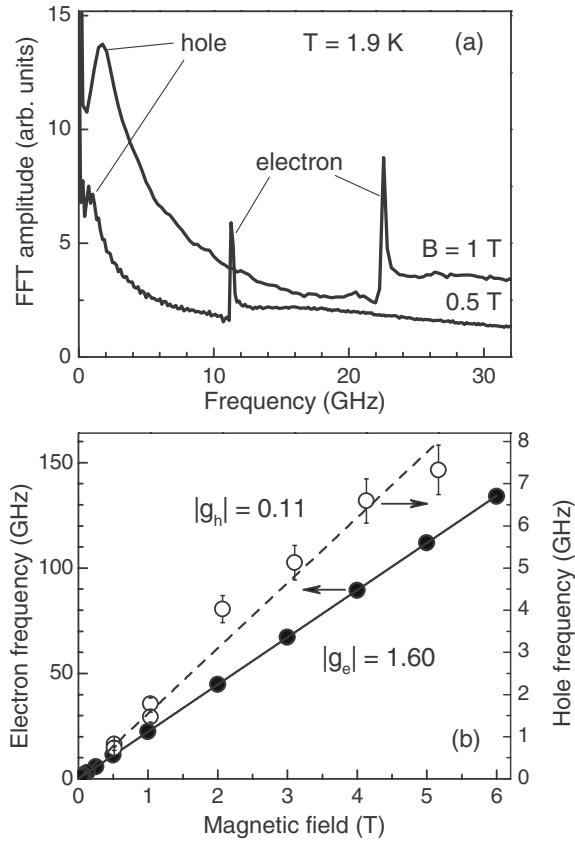


FIG. 8. (a) FFTs of the spin dynamics measured by degenerate pump probe at the trion resonance (1.5989 eV; see Fig. 7) for two different magnetic fields. (b) Magnetic field dependencies of electron and hole spin precession frequencies evaluated from the FFT analysis. Lines show linear interpolations of data points, whose slopes give the carrier g factors.

times for the moderate temperature increase from 1.9 to 6 K. For temperatures above 25 K it cannot be extracted from the data. Such a strong temperature dependence has also been reported for p -doped GaAs/(Al,Ga)As QWs.¹⁹ It has been explained by thermal delocalization of holes. Spin relaxation processes are significantly suppressed for localized holes only, but the spins of free holes relax very fast due to spin-orbit interaction. Our results on the hole spin coherence in CdTe-based QWs are in good qualitative and quantitative agreement with previously reported data for GaAs-based QWs. Therefore one can conclude that the mechanisms determining electron and hole spin dynamics are similar in II-VI and III-V heterostructures.

D. Control of resident carrier type by illumination

We used above-barrier illumination to change the type of resident carriers from holes to electrons. As one can see in Fig. 10 an increase in illumination power density to 6 W/cm² causes an amplitude enhancement of the fast oscillating electron contribution in the Kerr rotation signal by a factor of 40. In case of a low-density 2DEG the amplitude of the Kerr rotation signal is linearly proportional to the electron concentration, and therefore we conclude that the elec-

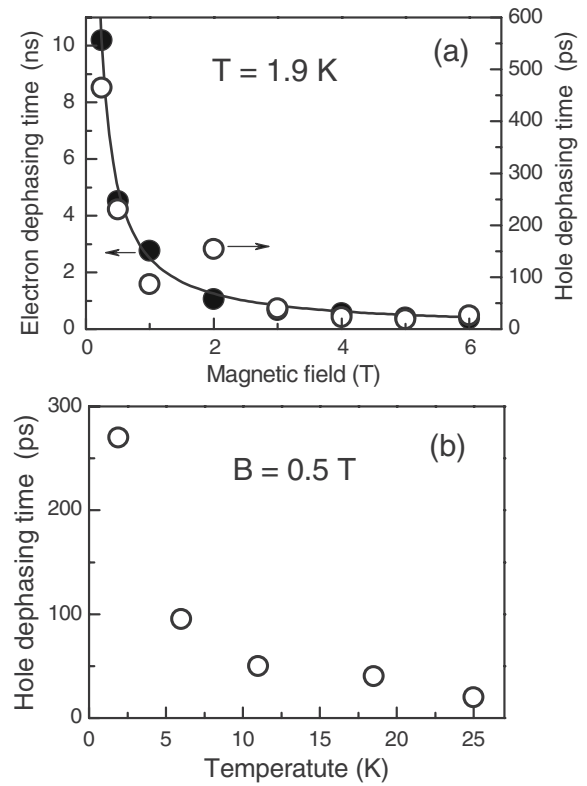


FIG. 9. Dephasing times for electrons $T_{2,e}^*$ (closed circles) and holes $T_{2,h}^*$ (open circles) as functions of (a) magnetic field and (b) temperature. Left and right scales in panel (a) are chosen to demonstrate that both electrons and holes are well described by a $1/B$ dependence given by the solid line, $\vartheta \approx 3.5^\circ$.

tron concentration in the QW increases 40 times.

The hole contribution also changes strongly under illumination. First, its amplitude relative to the electron signal decreases from $A_h/A_e=25$ without illumination down to 0.8 under strongest illumination (compare lower and upper curves in Fig. 10). This redistribution of amplitudes is clearly seen in the inset, where corresponding Fast Fourier transform (FFT) spectra are compared to each other. The hole peak has stronger integral intensity compared with the electron one without illumination, while a strong electron peak is visible under illumination only. Second, the hole spin dephasing time shortens under illumination from 240 ps down to 40 ps. The latter time coincides with the radiative recombination time of trions, meaning that under highest illumination (upper curve) the resident holes have disappeared in the QW, and the hole contribution to the Kerr rotation signal, seen as the small asymmetry relative to the zero signal line during the first three periods of electron spin precession, is due to photogenerated holes bound to T^- trions. In this regime we find the situation typical for n -type doped QWs.³⁰

Let us now turn to the surprising coexistence of the long-lived hole and electron spin beats that was observed without illumination (Figs. 7 and 10). Obviously it shows that both electrons and holes are present as long-lived resident carriers in the QW. The studied structure contains only one QW; therefore we suggest that the electrons and holes coexist in the same QW where they are separated spatially in the QW

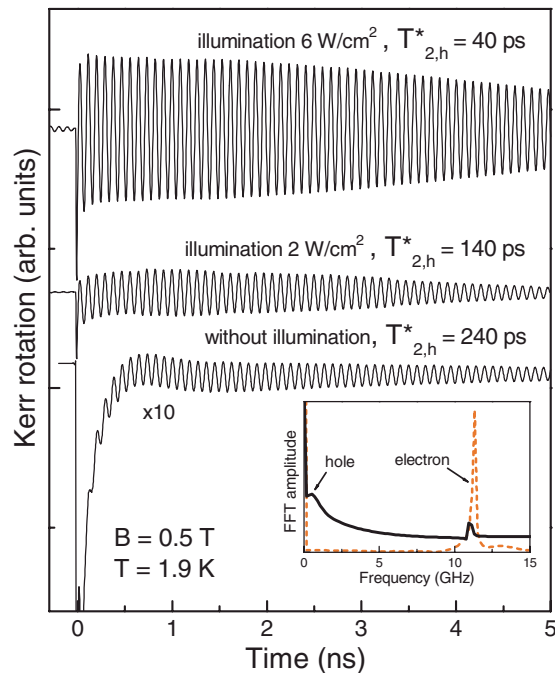


FIG. 10. (Color online) Kerr rotation signals for different powers of above-barrier illumination, which provides resident electrons in the quantum well. One-color pump-probe experiment with the laser energy at 1.5989 eV, resonant with the trion. Dephasing time of hole spin coherence $T_{2,h}^*$ is given in the panel. Fast Fourier transforms of Kerr signal with no illumination (solid line) and maximum illumination (dashed line) are shown in the inset.

plain. In other words, we have in this QW areas with dominant contribution from either resident electrons or resident holes. Most probably this is caused by an inhomogeneity of charge distribution provided by unintentional doping and

charge fluctuations on the structure surface. Such coexistence of two carrier types can be stable only at low carrier concentrations and is removed by illumination, which increases the concentration of background electrons.

IV. CONCLUSIONS

We have shown that in CdTe-based QWs with a low concentration of resident holes, corresponding to a regime when the hole-hole interactions can be neglected, long-living hole spin coherence can be observed. Hole spin dephasing times up to 500 ps were measured at a temperature of 1.9 K, shortening, however, considerably with increasing temperature up to 25 K. This behavior can be explained by acceleration of the spin relaxation for free holes compared with localized ones. These results are similar to the data reported earlier for GaAs-based QWs.¹⁹ We also observed in time-resolved pump-probe Kerr rotation spectra an unusual superposition of long-living spin beats from electrons and holes. The relative contributions of the electrons and holes could be tuned by above-barrier illumination in favor of the electrons. We explain this superposition by coexistence of both resident electrons and holes in the same QW but separated spatially in the QW plane. The pump-probe Kerr rotation technique is a method well suited for studying such situations and evaluating the relative concentrations of the resident carriers.

ACKNOWLEDGMENTS

The work was supported by the Deutsche Forschungsgemeinschaft, the Russian Foundation for Basic Research, the Ministry of Science and Higher Education (Poland) through Grant No. N202 054 32/1189, and the Foundation for Polish Science through Grant No. 12/2007.

¹*Spin Physics in Semiconductors*, edited by M. I. Dyakonov (Springer-Verlag, Berlin, 2008).

²*Semiconductor Quantum Bits*, edited by F. Henneberger and O. Benson (World Scientific, Singapore, 2008).

³*Semiconductor Spintronics and Quantum Computation*, edited by D. D. Awschalom, D. Loss, and N. Samarth (Springer-Verlag, Berlin, 2002).

⁴A. Greulich, R. Oulton, E. A. Zhukov, I. A. Yugova, D. R. Yakovlev, M. Bayer, A. Shabaev, Al. L. Efros, I. A. Merkulov, V. Stavarache, D. Reuter, and A. Wieck, *Phys. Rev. Lett.* **96**, 227401 (2006).

⁵A. Imamoglu, D. D. Awschalom, G. Burkard, D. P. DiVincenzo, D. Loss, M. Sherwin, and A. Small, *Phys. Rev. Lett.* **83**, 4204 (1999).

⁶I. A. Merkulov, Al. L. Efros, and M. Rosen, *Phys. Rev. B* **65**, 205309 (2002).

⁷*Optical Orientation*, edited by F. Meier and B. P. Zakharchenya (North-Holland, Amsterdam, 1984).

⁸ p type hole wave function has zero density on the nuclei which vanishes the contact hyperfine interaction.

⁹T. Flissikowski, I. A. Akimov, A. Hundt, and F. Henneberger,

Phys. Rev. B **68**, 161309(R) (2003).

¹⁰S. Laurent, B. Eble, O. Krebs, A. Lemaitre, B. Urbaszek, X. Marie, T. Amand, and P. Voisin, *Phys. Rev. Lett.* **94**, 147401 (2005).

¹¹D. Heiss, S. Schaeck, H. Huebl, M. Bichler, G. Abstreiter, J. J. Finley, D. V. Bulaev, and D. Loss, *Phys. Rev. B* **76**, 241306(R) (2007).

¹²B. D. Gerardot, D. Brunner, P. A. Dalgarno, P. Öhberg, S. Seidl, M. Kroner, K. Karrai, N. G. Stolz, P. M. Petroff, and R. J. Warburton, *Nature (London)* **451**, 441 (2008).

¹³J. Fischer, W. A. Coish, D. V. Bulaev, and D. Loss, *Phys. Rev. B* **78**, 155329 (2008).

¹⁴T. C. Damen, L. Viña, J. E. Cunningham, J. E. Shah, and L. J. Sham, *Phys. Rev. Lett.* **67**, 3432 (1991).

¹⁵Ph. Roussignol, R. Ferreira, C. Delalande, G. Bastard, A. Vinatieri, J. Martinez-Pastor, L. Carraresi, M. Colocci, J. F. Palmier, and B. Etienne, *Surf. Sci.* **305**, 263 (1994).

¹⁶B. Baylac, T. Amand, X. Marie, B. Dareys, M. Brousseau, G. Bacquet, and V. Thierry-Mieg, *Solid State Commun.* **93**, 57 (1995).

¹⁷B. Baylac, X. Marie, T. Amand, M. Brousseau, J. Barrau, and Y.

- Shekun, Surf. Sci. **326**, 161 (1995).
- ¹⁸X. Marie, T. Amand, P. Le Jeune, M. Paillard, P. Renucci, L. E. Golub, V. D. Dymnikov, and E. L. Ivchenko, Phys. Rev. B **60**, 5811 (1999).
- ¹⁹M. Syperek, D. R. Yakovlev, A. Greilich, J. Misiewicz, M. Bayer, D. Reuter, and A. D. Wieck, Phys. Rev. Lett. **99**, 187401 (2007).
- ²⁰I. A. Yugova, A. A. Sokolova, D. R. Yakovlev, A. Greilich, D. Reuter, A. D. Wieck, and M. Bayer, Phys. Rev. Lett. **102**, 167402 (2009).
- ²¹G. V. Astakhov, V. P. Kochereshko, D. R. Yakovlev, W. Ossau, J. Nürnberger, W. Faschinger, G. Landwehr, T. Wojtowicz, G. Karczewski, and J. Kossut, Phys. Rev. B **65**, 115310 (2002).
- ²²G. V. Astakhov, D. R. Yakovlev, V. P. Kochereshko, W. Ossau, W. Faschinger, J. Puls, F. Henneberger, S. A. Crooker, Q. McCulloch, D. Wolverson, N. A. Gippius, and A. Waag, Phys. Rev. B **65**, 165335 (2002).
- ²³E. A. Zhukov, D. R. Yakovlev, M. Bayer, M. M. Glazov, E. L. Ivchenko, G. Karczewski, T. Wojtowicz, and J. Kossut, Phys. Rev. B **76**, 205310 (2007).
- ²⁴G. Bartsch, M. Gerbracht, D. R. Yakovlev, J. Blokland, P. C. M. Christianen, E. A. Zhukov, N. A. Gippius, G. Karczewski, T. Wojtowicz, J. Kossut, J. C. Maan, and M. Bayer (unpublished).
- ²⁵A. A. Sirenko, T. Ruf, M. Cardona, D. R. Yakovlev, W. Ossau, A. Waag, and G. Landwehr, Phys. Rev. B **56**, 2114 (1997).
- ²⁶G. V. Astakhov, D. R. Yakovlev, V. V. Rudenkov, P. C. M. Christianen, T. Barrick, S. A. Crooker, A. B. Dzyubenko, W. Ossau, J. C. Maan, G. Karczewski, and T. Wojtowicz, Phys. Rev. B **71**, 201312(R) (2005).
- ²⁷G. Finkelstein, H. Shtrikman, and I. Bar-Joseph, Phys. Rev. B **53**, 12593 (1996).
- ²⁸G. V. Astakhov, V. P. Kochereshko, D. R. Yakovlev, W. Ossau, J. Nürnberger, W. Faschinger, and G. Landwehr, Phys. Rev. B **62**, 10345 (2000).
- ²⁹R. A. Sergeev, R. A. Suris, G. V. Astakhov, W. Ossau, and D. R. Yakovlev, Eur. Phys. J. B **47**, 541 (2005).
- ³⁰D. R. Yakovlev and M. Bayer, in *Spin Physics in Semiconductors*, edited by M. I. Dyakonov (Springer-Verlag, Berlin, 2008), Chap. 6, p. 135.